Advances in Science and Technology Research Journal

Advances in Science and Technology Research Journal, 2025, 19(6), 223–234
https://doi.org/10.12913/22998624/201451
ISSN 2299-8624, License CC-BY 4.0

Received: 2024.11.18
Accepted: 2025.04.15
Published: 2025.05.01

Limits of the variability of the operating states of the ultralight autogyro engine

Piotr Andrzej Jakliński[1], Karol Jan Ścisłowski[1,2*]

[1] Department of Thermodynamics, Fluid Mechanics and Aircraft Propulsion Systems, Lublin University of Technology, Poland
* Corresponding author's e-mail: k.scislowski@pollub.pl

ABSTRACT

The publication presents an analysis of the operating conditions of the propulsion system of an ultralight autogyro during flights of various lengths and dynamics. This analysis is aimed at demonstrating the limits of variability of engine operation to determine the boundary conditions of aircraft engine operating conditions in actual operation. This parameter, in turn, will enable the effective use of the advantages of aircraft hybridization depending on the type of mission. The research data was collected from 10 different flights of the TERCEL autogyro. MAP, RPM, flight altitude, horizontal and vertical speed, etc. were extracted from the on-board FDR (Flight Data Recorder) and then analyzed. The flights were classified as short SF (< 30 min) and long LF (> 30 min). The defined engine operating states include steady-state and transient engine operation, IDLE, low load (LL), high load (HL), and wide-open throttle (WOT), as well as acceleration and deceleration. The analysis of the data shows that for the short flights, the share of steady state is about 80% and increases to more than 90% for the long flights. For the short flights, the share of acceleration accounts for about 60% of transient states and also increases to more than 65% for the long flights. For the short flights, IDLE, LL and WOT have a fairly significant share and amount to 32%, 36.1% and 7.5%, respectively, while they are increasingly marginalized by the increasing share of HL as the flight lengthens. For the long flights, The share of HL was almost 70%.

Keywords: rotorcraft, gyroplane, IDLE, WOT, steady state, acceleration, deceleration, engine load, operating states, hybrid propulsion.

INTRODUCTION

Reciprocating internal combustion engines are still widely used in light aviation. Current trends indicate that they will continue to be used to power manned and unmanned aircraft for a long time to come and will continue to be researched and developed [1–3]. When analyzing the development of the automotive industry and aviation, it can be concluded that the solutions used in automotive vehicle propulsions are also being adapted to light aviation over time [4, 6]. This fact means both improving the functionality of propulsion systems and reducing emissions of harmful exhaust components [5, 7]. Carbureted power systems are being replaced by electronic fuel injection [7, 8], and turbocharging is being used to increase maximum power and latitude with no significantly increased aircraft weight [9, 11]. The accelerating electrification of land transportation is the fact so it is clear that in the future it will also apply to aviation [12, 13]. Electric propulsion systems are already in use in, for example, motorized gliders [15] motor-paragliders or drones, but they have a relatively low flight duration [10]. This is due to the low energy density of the batteries currently in use the large weight of which is the greatest limitation in the electrification of aviation [13, 14]. Therefore, it can be expected that an intermediate solution will be hybrid systems [9, 19] in which the electric motor will support the internal combustion engine in higher power demand or in states of temporary changes in operating conditions will be capable of maintaining a stable operating point of the internal

combustion engine [15, 16]. There are also considered solutions of series systems where the internal combustion engine drives only the electric generator [17, 18], but such systems show the greatest efficiency in aircraft like motor gliders. Hybrid solutions do not require a large energy storage and simultaneously show a considerably increased total power and better flexibility of the propulsion system and better dynamic operation. Research is already underway to apply hybrid propulsion systems to light aviation [19]. Building a functional hybrid propulsion system requires designing a control system that will, according to demand, provide smooth control of power distribution from electric and internal combustion engines. Such a system must analyze the operating conditions of the propulsion system and flight parameters in real time to select the most favorable power distribution strategy similar to automotive FHEV (full hybrid electric vehicles) systems [21], which is of particular importance for unmanned vessels where human control of individual systems is reduced to a minimum [23–25].

In order to determine the prerequisites for the construction of a power distribution system, it is necessary to define the operating conditions of an aircraft propulsion system. The previous studies have defined the main differences in powertrain operation between reciprocating aircraft and automotive propulsion systems [16]. It was shown that the aircraft engine operates with a much higher average load, and transient operating conditions occur rarely. The questions then arise: Will the different operating profile of the aircraft engine significantly reduce the advantages observed in hybrid vehicles, and if so, will the conditions of the flight being conducted, i.e. the type of mission, affect the benefits obtained, and how large will this effect be?

In order to answer these questions, it is necessary at first to determine the range of variation in the operating conditions of the aircraft engine depending on the mission, which is what this work sought to establish.

Scope of research

The research has determined the boundaries of aircraft engine operating states, i.e. the share of individual aircraft engine operating states in different flight durations, conditions and types of missions. If these relationships are specified under real operating conditions, the differences in the operating conditions of the propulsion system of an ultralight aircraft and their causes can be correctly defined. By indicating and defining the recorded differences, the most efficient control of the hybrid propulsion system can be defined and consequently the advantages due to its application in the aircraft can be taken.

Understanding values such as flight time, engine load, as well as the steady and transient operating states of the engine is crucial for assessing the feasibility of hybrid propulsion systems and estimating the associated benefits. Flight duration affects engine operating states and, consequently, fuel consumption and energy efficiency. For hybrid propulsion systems, optimizing flight time can lead to better energy resource management, which is essential for achieving environmental, economic, and operational benefits (performance, range).

The engine load influences its efficiency, fuel consumption, as well as noise, heat emissions, vibrations, and the wear rate of components. In hybrid propulsion systems, managing engine loads can help optimize the performance of both the internal combustion engine and the electric motor, leading to more efficient resource utilization. The steady and transient operating states in hybrid propulsion systems alter the ability to manage energy effectively. Understanding the range of these values (as analyzed in this study) is key to identifying the ways to maximize the benefits related to fuel savings and emission reductions while balancing the costs of hybridization, such as weight, expenses, and other associated factors.

RESEARCH OBJECT AND METHODOLOGY

Research object

The object of the study was an ultralight Tercel-type gyroplane, manufactured by the AVIATION Artur Trendak company (Fig. 1). The technical data of the aircraft are shown in Table 1. The aircraft was powered by an AAT 912 RSTi 4-cylinder, gasoline piston engine. It is a commonly used engine in ultralight aviation, the Rotax 912 UL, modified by the manufacturer of the analyzed autogyro by adding turbocharging. The technical data of the propulsion unit is shown in Table 2. The aircraft was also equipped with an A&ATech FDR (flight data recorder) on-board recorder of flight parameters and propulsion system operating conditions to record measurement data at a sampling rate of 10 Hz.

Figure 1. Tercel gyroplane

Table 1. Technical data of the Tercel gyroplane

Main rotor diameter	8.60 m
Overall length (without rotor)	5.04 m
Overall height	2.35 m
Hull width	2.35 m
Maximum takeoff weight	560 kg
Dead weight	295 kg
Propeller	Kaspar Aero 2/3 LT
Reducer ratio	2.43:1

Table 2. Technical data of the AAT 912 RSTi engine

Cylinder system	4, boxer
Engine displacement	1 211 cm^3
Bore	79.5 mm
Stroke	61 mm
Compression ratio	9.0:1
Fuel supply system	Multipoint indirect injection
Max. power	140 HP (103 kW) / 5 800 RPM
Nominal power	125 HP (92 kW) / 5 500 RPM

Research methodology

In order to determine the correlations between the incidence of particular aircraft engine conditions and the conditions of the flight conducted, i.e. the type of mission, the measurement data obtained during flights of different lengths and dynamics were compared and analyzed.

The values of parameters, such as the average engine load, the range of rotational speeds and loads used, and the correlations that occur between them depending on the flight conditions such as flight time, speed variation, altitude, etc. were analyzed.

Selection and analysis of the measurement results

The measurement data from the flights of different duration, altitude and cruise speed were selected for analysis. Attention was paid to ensure that each data sequence included a complete flight with all its stages the propulsion system worked, i.e. engine warm-up, taxiing, takeoff, cruise and landing. The analysis was based on the data recorded during 10 diversified flights meeting the above criteria.

Due to the limited resolution of the measurement of parameters, such as intake manifold pressure (MAP) and speed (RPM), data filtering was performed by averaging the 3 closest measurement points (averaging range – 300 ms). This made it possible to cancel out noise in the form of spikes in the time derivative of the measured parameters, which will be important for further stages of analysis, especially for classification of transient states. The collected results enabled a comparative analysis of the contribution of different states of propulsion system operation during short and long flights.

For the purpose of analysis, flights were classified into two groups, i.e. short flights and long flights. The recorded flights were classified as short if the total duration of propulsion system operation (including warm-up, taxiing, etc.) did not exceed 30 minutes. Those lasting more than 30

minutes were classified as long flights. The percentage of engine operating points such as steady and transient states, IDLE, low-, medium- and heavy-load operation, and full-load WOT were determined by setting limits for each parameter:

- IDLE – speed below 2000 RPM,
- low load – power utilization ratio (PCR) below 0.5,
- kigh load – power utilization ratio reaches values in the range of 0.5 < PCR < 1.0
- WOT – power utilization ratio reaches values above 1.0.

The various engine operating states were classified based on parameters read by the engine control unit (ECU), such as MAP intake manifold pressure and RPM engine speed.

Analysis of the results

During the study, 10 flights were analyzed and the total recording time of the collected data (time of all flights) was 7 hrs and 29 min. The shortest recorded flight was 12.6 min, whereas the longest one was 108.2 min. The flights were conducted up to an altitude of 1461.6 m and a maximum speed of 189.4 km/h.

MAP intake manifold pressure and RPM speed were taken as the main parameters determining the operating conditions of the powertrain. The analysis of the variation of these parameters enabled to classify static and dynamic operating states of the engine, using a method consistent with the previous analyses [26]. Such operating points were defined as steady states at which the one-second change in the MAP and RPM parameters did not exceed 1% of the useful range. Figure 2 shows the method of steady-state classification.

For speed, the useful range was determined between the idle speed (1800 RPM) and the maximum speed (5500 RPM). The useful range of intake manifold pressure was taken as the range between 0.30 bar (pressure at no-load idling speed) and 1.35 bar (intake system pressure at rated power). When classifying the engine operating points according to this methodology, it was found that transient conditions occurred for a total of 10.6% of the total operating time in all flights.

Another parameter determining the operating conditions of the propulsion system was the power utilization ratio PCR. It was determined in a manner consistent with the previous analyses [26] in line with the following formula:

$$P_{CR} = \frac{RPM_i - RPM_{min}}{RPM_{nom} - RPM_{min}} \cdot \frac{MAP_i - MAP_{idle}}{MAP_{nom} - MAP_{idle}} \quad (1)$$

where: RPM_i – rotational speed at the analyzed operating point, RPM_{min} – minimum idle speed (1800 RPM), RPM_{nom} – rotational speed at nominal power (5500 RPM), MAP_i – intake air pressure at the analyzed operating point, MAP_{IDLE} – intake air pressure at no-load idle speed (0.30 bar), MAP_{nom} – intake air pressure at nominal power (1.35 bar).

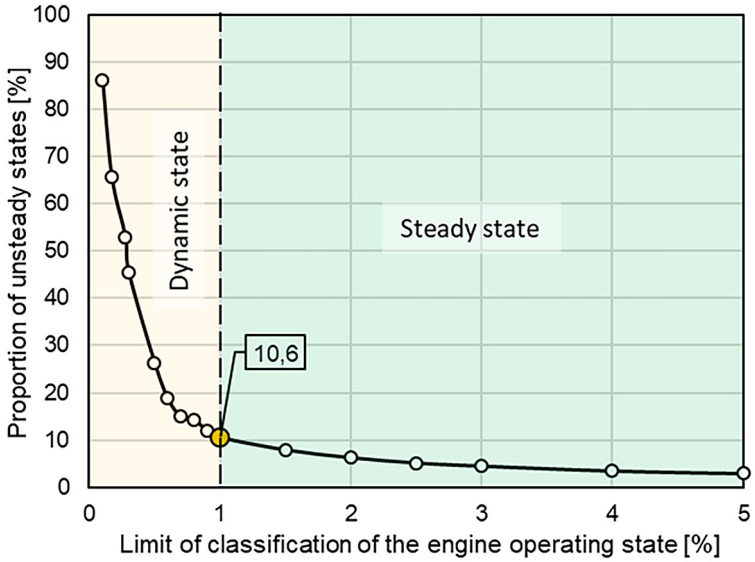

Figure 2. Proportion of the dynamic operating states for the assumed classification criteria

According to formula (1), the mean value of the power utilization ratio (MPCR) was determined for all flights. Figure 3 illustrates the relationship between the MPCR value and total flight duration. An extrapolation of the average value using a logarithmic function was performed up to a limit of 300 min, which is the predicted maximum duration of horizontal flight, and a value of about 0.7 was obtained.

There is a clear correlation between the average value of the power utilization factor and flight duration. As the flight is longer, MP¬CR increases. This is due to the smaller percentage of time in longer flights of stages such as warm-up, descent and landing. The opposite tendency can be seen for the standard deviation of the power utilization ratio (σPCR). Figure 4 shows the value of the standard deviation of the power utilization ratio σPCR for the entire flight. The graph below clearly shows that the PCR value is characterized by greater variability in shorter flights, while the power system's exertion is more stable as the flight is longer. When extrapolated to the 300-minute limit, a value below 0.2 was obtained.

According to the analyses based on the previous studies, in this case, too, the aircraft engine exhibits operation mainly in two ranges of load and speed, which can be quite clearly divided into the area of low and high loads (Fig. 5). The low loads (RPM 1000–2000 1/min, MAP 0.35–0.50 bar) occur mainly during engine warm-up, taxiing, or lowering flight, e.g. before landing. The high engine loads (RPM 4500–5500 1/min, MAP 1.0–1.2 bar) are typical for steady-state flights or climb. In a small range, full engine load (MAP > 1.2 bar) is also used, but this occurs mainly during takeoff and in the initial stages of climb.

In order to better illustrate the differences in engine operating conditions from flight to flight, the distributions of speeds and loads were analyzed. All flights were marked with consecutive letters of the alphabet, ranking them from shortest to longest. Table 3 contains the symbols used and the most important values characterizing the individual flights analyzed.

Figure 6 shows the ranges of rotational speeds that occur during each flight. It is noticeable that the average engine speed increases as flight is longer. The median rotational speed in flights F–J lies above the mean value, which means that the most of the engine operating ranges is shifted toward higher rotational speeds. The distribution of the measured rotational speeds also decreases

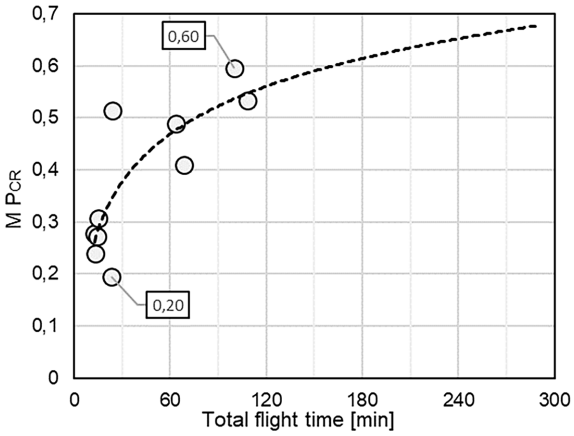

Figure 3. Average power consumption ratio MP_{CR} for flights of different durations

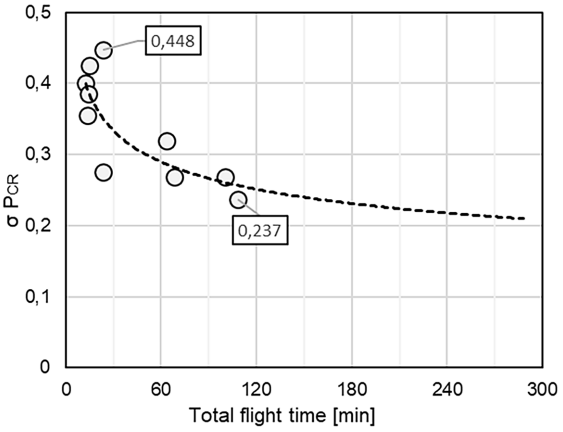

Figure 4. Standard deviation of the power consumption ratio σP_{CR} for flights of different durations

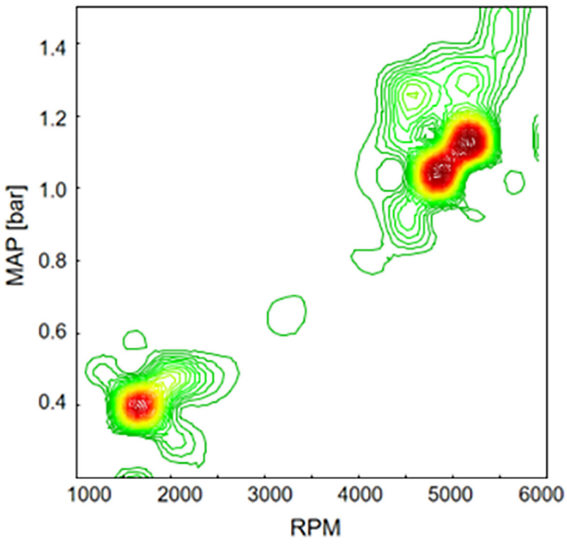

Figure 5. Contour map of the engine operating points density for the research gyroplane during all recorded flights

Table 3. Symbols and parameters of the recorded flights

Flights	Flight symbol	Flight time [mi]	P_{CR} avg. [-]	Engine speed avg. [RPM]	MAP avg. [bar]
Short flights	A	12.6	0.278	3 181	0.73
	B	13,4	0.239	2 858	0.69
	C	14.4	0.272	2 942	0.72
	D	20.4	0.308	3 120	0.79
	E	23.7	0.196	2 904	0.65
	F	23.7	0.513	3 814	0.93
Long flights	G	63.6	0.488	3 943	0.87
	H	68.4	0.410	4 025	0.87
	I	100.2	0.595	4 552	1.05
	J	108.2	0.534	4 227	1.07

as flight is longer. For Flight I and Flight J, the measurement points recorded during warm-up and landing, due to their relatively small number, were interpreted as "outliers", i.e. statistically insignificant in the analysis of flight conditions. The average speed was lowest for Flight B (13.4 min) at 2858 RPM, while the highest one for Flight I (100.2 min) was 4552 RPM.

Figure 7 shows the range of the recorded aircraft engine load (MAP) in individual flights. The distribution of the recorded values is similar to the one for speed. For the short flights (A÷E), lasting less than 15 minutes, the average load is higher than the median, which means that more than half of the total time is accounted for by points such as warming up and taxiing. The smallest average MAP value was recorded for flight E (0.65 bar), while the largest one was recorded for the longest flight J (1.07 bar). All operating points where the speed was below 2000 RPM were classified as idle. The largest share of IDLE in the entire flight (24–44%) was registered for the short flights. For the long flights, the share of idling was within 8.5%. It should be noted that the IDLE operating time for all measurements was within the range of 3–10 min per flight.

The percentage of engine operating time at full load (WOT) was 3.22%. The total engine operating time at full load for each of the recorded flights was in the range of 0.4–4.0 min. Figure8 shows the percentage of the engine operating time at idle and full load conditions for all recorded flights. It is noticeable that there is a clear tendency for the proportion of these states to decrease as the flight lengthens. For 300 min, the predicted operating times at IDLE and WOT are

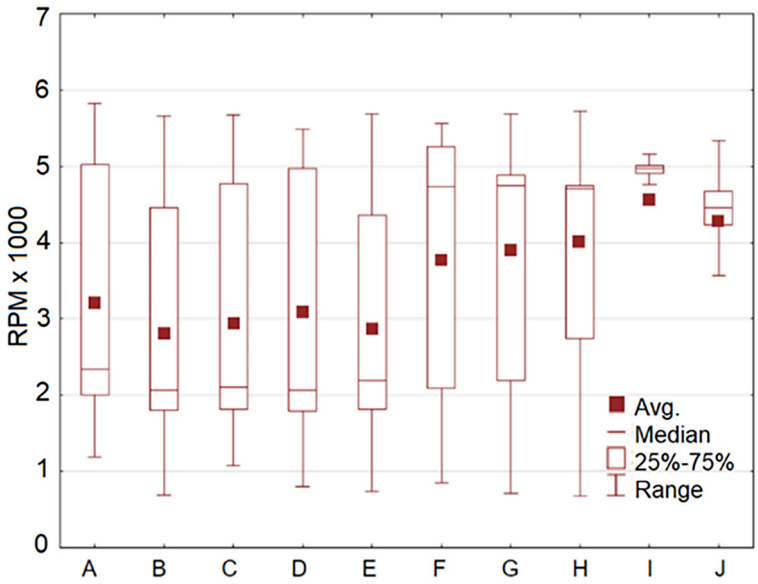

Figure 6. Range of the recorded speeds in all analyzed flights

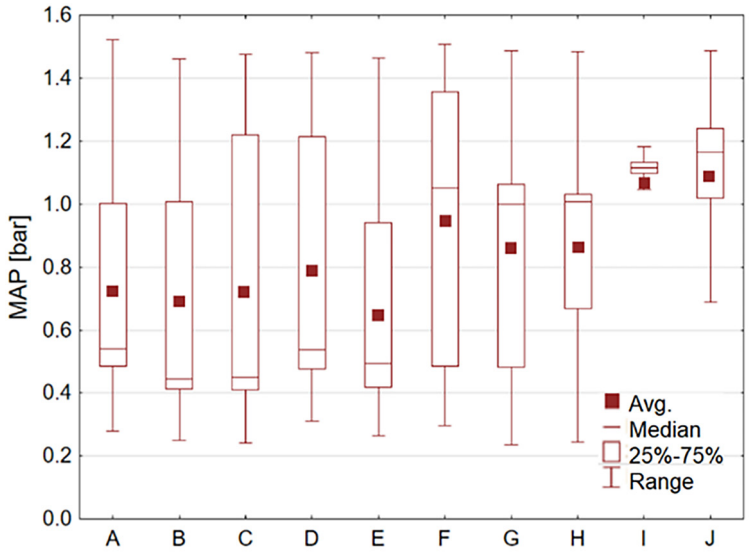

Figure 7. Range of the engine loads in all analyzed flights

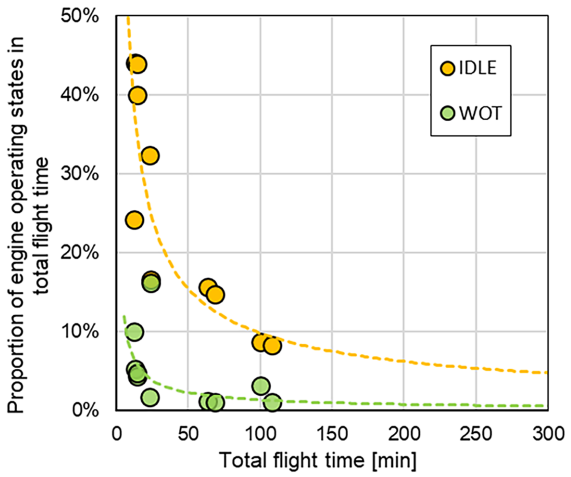

Figure 8. Share of IDLE and WOT in the total time of individual flights

approx. 4% and 1%, respectively. The dynamic operating states of the internal combustion engine are potential conditions for the most effective use of the advantages of hybrid propulsion, so determining their share and extent of occurrence is the main issue of the analysis. Their share in the total time of individual flights was determined in accordance with the method of classifying engine operating states presented in the previous publication. The highest share of dynamic states was registered during the shortest flight A (41.3%) – the red point in Fig. 9. This value is a clear outlier from the other flights in a similar time interval (B–F) for which the share of dynamic operating states was in the range of 20.3–26.3%. As the flight lengthens, the share of transient states decreases, reaching the lowest value of 5.79% for Flight I. It can be assumed that for 300 min. the share of transient states will be about 3.5%. Fig. 10 shows the distribution of the occurrence of dynamic operating points in all recorded flights. The results of the earlier analyses for larger aircraft show that the highest density of the occurrence of dynamic states was recorded at speeds in the range of 1500–3000 RPM and MAP of 0.3–0.6 bar. This is the range in which power most often increases after engine warm-up and speed adjustments during taxiing when engine power is frequently changed. Another area of a higher occurrence of dynamic states is the-medium-to-heavy-load range of 4200 ÷ 5800 RPM and MAP of 0.9–1.5 bar.

The following diagrams (Fig. 11 and Fig. 12) show the distributions of the dynamic

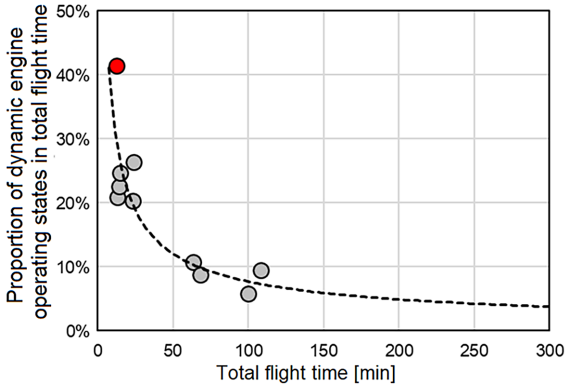

Figure 9. Share of the transient engine states in for the flights of different durations

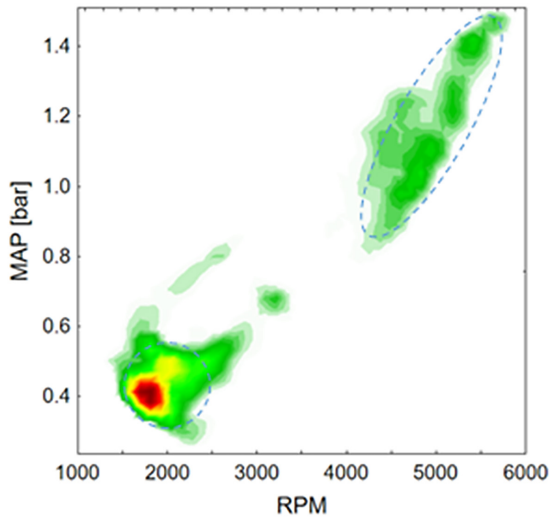

Figure 10. Distribution of the occurrence of the dynamic engine operating states for all analyzed flights

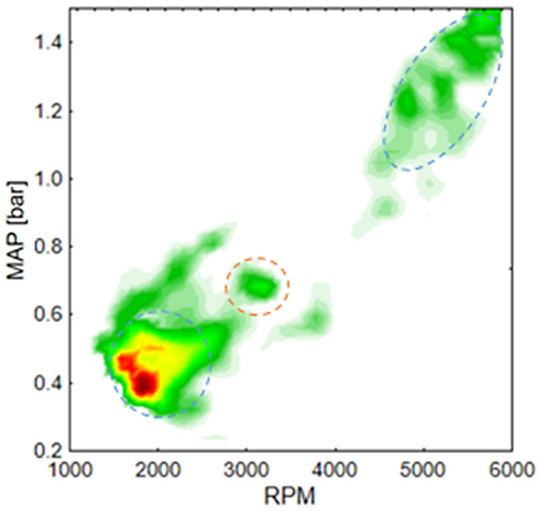

Figure 11. Distribution of the transient engine states for the short flights

engine operating states by short flights and long flights. It can be seen that for the short flights the transient states occur mainly in ranges of low speed and load. This is probably due to the fact that in missions such as training flights, a significant part of the entire flight is occupied by taxiing on the runway, while climbing occurs at high loads, but under relatively stable conditions. For the long flights, transient states occur over a much larger area in the range of high load and speed (Fig. 11). For low speed and low loads, they are similar although not identical to those of short flights. One can also see a larger share of transient states in the medium load range around 3000 RPM and 0.6–0.7 bar MAP – the orange line.

Figure 13 shows the distribution of the occurrence of the dynamic operating states. The dynamic states are divided into positive – (acceleration), marked in red (dRPM/dt > 0), and negative (deceleration), marked in green (dRPM/dt < 0).

For the positive dynamic states, the average speed is 3205 RPM, with a standard deviation of σRPM = 1397 RPM. The negative states occur at speeds higher by an average of 3.6% of the useful range, amounting to 3377 RPM, σRPM = 1385 RPM. The mean engine load (MAP) and its deviation obtain very similar values for the positive states – 0.83 bar (σMAP = 0.40 bar) and 0.81 bar (σMAP = 0.42 bar) for the negative states.

Figure 14 shows the percentages of the steady- and transient-state times obtained in the short and long flights. For the short flights,

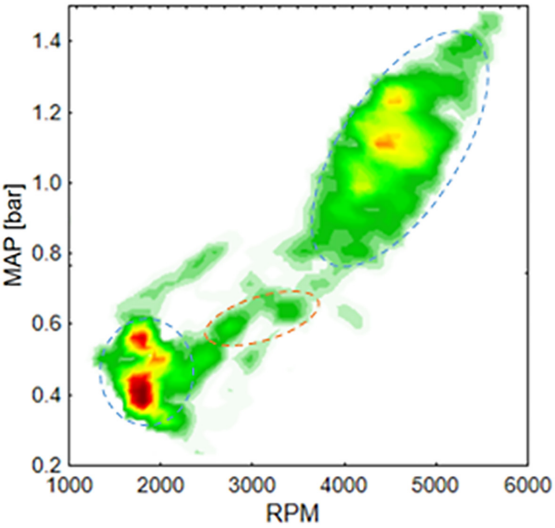

Figure 12. Distribution of the transient engine states for the long flights

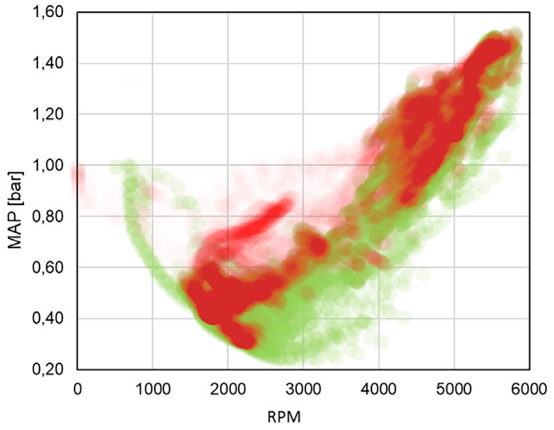

Figure 13. Distribution of the incidence of the dynamic negative-deceleration (green) and dynamic positive-acceleration (red) engine operating points

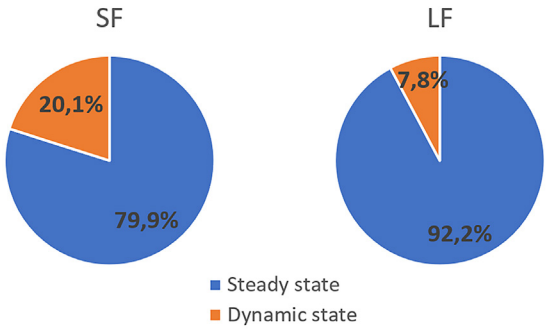

Figure 14. Share of the static and dynamic engine states in the short and long flights

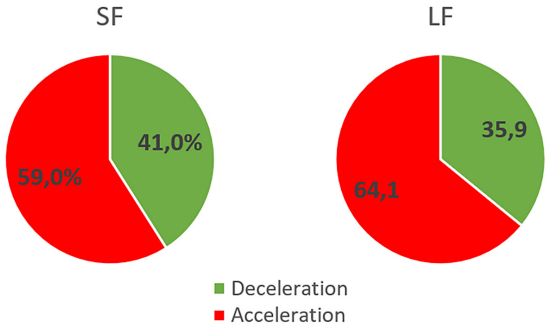

Figure 15. Share of acceleration and deceleration in the short and long flights

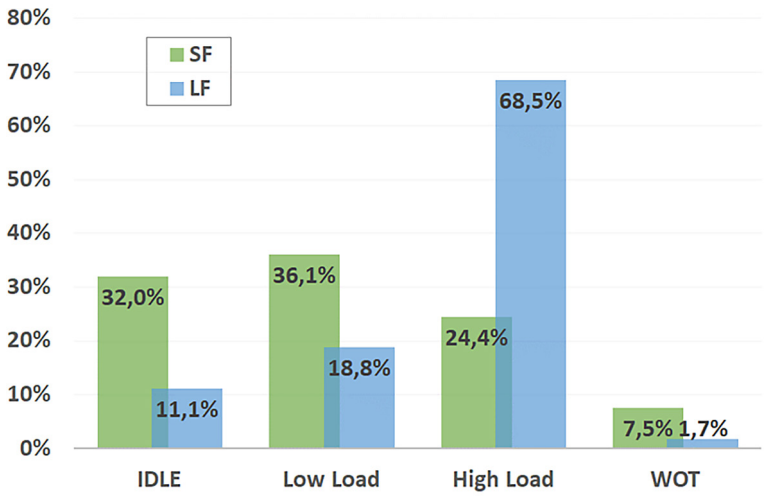

Figure 16. Share of the individual engine operating states in the short and long flights

steady states account for 79.9% of flight time, while for the long flights, steady states occur 12.3 p.p. longer and account for as much as 92.2% of flight time. In the short flights, the transient states account for 20.1% of flight time and in the long flights only 7.8% of flight time. Figure 15 shows the percentages of the positive (acceleration) and negative (deceleration) transient /dynamic states obtained in the short and long flights. For the short flights, acceleration accounts for 59% of the transient flight time, and deceleration 41%. For the long flights, the share of acceleration increased by 5.1 p.p. to 64.1% of the transient flight time, and thus the share of deceleration decreased to 35.9%. Regardless of the length of flights, the share of acceleration was recorded to be greater than the share of deceleration. Figure 16 shows a comparison of the share of the selected engine operating states during the short and long flights. Such a classification highlights the differences in the loads used due to flight duration. For the short flights, an idle of 32% and a low load of 36.1% together accounted for 68.1% of total engine operation time and they were significantly higher than those obtained for the long flights. The same power utilization ranges for the long flights are 11.1% and 18.8%, respectively, and together account for only 29.9% of the engine's operating time.

In addition, in both short and long flights, the share of idling is several percentage points lower to the share of low load. They are 32% and 36.1% in the short flights and 11.1% and 18.8% in the long flights, respectively. Similarly to IDLE and LL, the share of WOT for the short flights is significantly higher than for the long flights and is as high as 7.5% or more than 4 times higher than for the long flights when only 1.7% was recorded.

An important difference is the share of high load HL. In the long flights, it is as high as 68.5%, a value almost three times higher than 24% obtained in the short flights.

CONCLUSIONS

The correlation analysis between flight time and propulsion system operating conditions carried out in this study has made it possible to determine the share of individual propulsion system operating states for the analyzed aircraft. The results of the study indicate that for short-range flights, steady states account for about 80% of the total flight time, while for long-range flights, it is already more than 92%. Further extension of flight time (up to maximum range) should, therefore, lead to an increase in the share of steady states above 92%.

The remainder are transient/dynamic states. The occurrence of these transient states, characterized by variations in engine load, rotational speed, and power utilization factor, plays a key role in assessing the potential benefits of hybrid propulsion. By analyzing the frequency and intensity of these changes, it is possible to identify operational phases where hybridization could provide the most significant advantages. Managing transient states effectively allows for optimization of power distribution, which can lead to better fuel efficiency and reduced emissions while ensuring stable system performance. In terms of power distribution management for hybrid propulsion in similar aircraft, it is crucial to define the frequency of engine transient states and identify acceleration and deceleration. When analyzing the results, it was observed that as flight is longer, the share of positive transient states, i.e. acceleration increases. For long flights, this share is 5.1 p.p. higher than in short ones, so it seems that as flight is longer and longer, this share will further increase.

In the analysis above, attention was also paid to the share of characteristic engine operating states such as IDLE, WOT or the average value of the MPCR power utilization factor and its standard spread σPCR as well as the share of low and high loads. The short flights were characterized by a high proportion of idling, accounting for 25–45% (average 32%) of the total flight time that covers such stages as engine warm-up and taxiing. For hybrid propulsion control, the range of the use of low loads can also provide a partial recharging of energy stores before takeoff. By correlating these data to the operating conditions map, potential benefits from using electric propulsion support in this range can be expected, which could compensate for temporary increases in transient power demand and recharge batteries during an engine warm-up.

The percentage of WOT also shows a dependence on flight duration that decreases as flight time is longer. The share of WOT reached from 17% for the shortest flights to about 1% for the longest ones. The obtained average share of 7.5% for the short flights is more than four times higher than the one for the long flights (1.7% on average). WOT, too, is a range of operation in which propulsion hybridization can bring potential benefits. Despite the higher share of maximum load in the short flights, larger average values of the power utilization factor were obtained for the longer flights, reaching the highest value of MPCR = 0.59 for an "I" flight lasting 100.2 minutes.

It seems that the differences described are mainly due to the time of the use of the large load for long, fixed flights. The longer the flight, the greater the share of precisely the large engine load which affects the magnitudes of the other states by making them lower. In short flights, such as training flights, a large share is taken up by takeoff and climb (WOT) as well as descent and landing (low load).

The stability of operating conditions was given, among other things, as the standard deviation of the PCR parameter for each flight. The value of the standard deviation decreased as the flight became longer. Similar results of the variability of engine operating conditions were obtained from the analysis of the time derivative of RPM and MAP intake manifold pressure and the values of their standard deviation (σMAP and σRPM). A correlation was confirmed between the share of transients during the analyzed flights and the relative value of the standard deviation of the PCR, RPM and MAP parameters. With increasing flight length, a tendency to shift the highest frequency of transients to the range of high loads can be observed. We shows that in the short flights (< 30 min of engine operation), most transients occur in the low load and low speed range, i.e. mainly during taxiing, changes in airspeed, turns or changes in climb and descent speeds which, due to the short flight time, make up a relatively large part of it. The short flights, e.g. training flights with a large proportion of both climb and approach to landing which, despite the extremely different load on the engine are highly uniformal (stable). For the longer flights, the percentage of taxiing is lower. During flight, the engine usually operates in the high load range, so the occurrence of

changes in operating conditions also statistically moves into the limits of this range.

This analysis unequivocally confirms that the type of mission and flight time have a significant impact on the distribution and share of various ranges of load and speed of the aircraft engine. The occurrence of engine transient states is closely dependent on flight time, and these transient states during the analysis can be diagnosed by both the time derivatives of the MAP, RPM and PCR parameters and their standard deviation, keeping the convergence of results and conclusions within an acceptable range. This analysis can be extended to defining individual flight stages and regarding the operating conditions of the propulsion system.

REFERENCES

1. Geca M, Czyż Z, Sułek M. Combustion Engines, CE-2017-202 Diesel engine for aircraft propulsion system, 2017; 169(2), 7–13, doi: 10.19206/CE-2017-202.
2. Czarnigowski J, Jakliński P, Ścisłowski K, Rękas D, Skiba K, The use of a low frequency vibration signal in detecting the misfire of a cylinder of an aircraft piston engine, no. August 2022; 2023, doi: 10.4271/2020-01-202.
3. Jakliński P, Czarnigowski J, Ścisłowski K. Analysis of the operating conditions of the ASz-62IR engine during flight, Advances in Science and Technology Research Journal 2024; 18(8): 56–72. doi: 10.12913/22998624/192699.
4. Jakliński P. The influence of the ignition control on the performance of an aircraft radial piston engine, Combustion Engines 2019; 177(2), 60–65, doi: 10.19206/CE-2019–211.
5. Selvaraju N. A Low-Cost Selective Catalytic Reduction System for Diesel Engine Oxides of Nitrogen Control, Technology Innovation in Mechanical Engineering, no. June, 2022; doi: 10.1007/978-981-16-7909-4.
6. Czarnigowski J, Jakliński P, Zyska T, Klimkiewicz J, Wendeker M. Analiza wpływu przepisów i standardów na konstrukcję elektronicznego systemu zapłonowego lotniczego silnika tłokowego, Logistyka. 2014; 6, 2869–2876.
7. Czarnigowski J, Jakliński P, Karpiński P. Effect of ignition advance angle offset in a dual ignition system of a large aircraft piston engine, Int. J. Engine Res., Jun. 2022; 24(12), 4537–4552, doi: 10.1177/14680874221103711.
8. Czarnigowski J, Jakliński P, Zyska T. Analysis of influence of legal requirements on the design of electronic ignition system for aviation piston engine, Journal of KONES. 2017; 24(1), 91–100, doi: 10.5604/01.3001.0010.2801.
9. Jakliński P, Analysis of the dual control system operation during failure conditions, Eksploat. i Niezawodn., 2013; 15(3), 266–272,
10. Rohacs J, Kale U, Rohacs D. Radically new solutions for reducing the energy use by future aircraft and their operations, Energy, 2022; 239, 122420. doi: 10.1016/j.energy.2021.122420.
11. Czarnigowski J, Skiba K, Rękas D, Ścisłowski K, Jakliński P. Bench Tests for Exhaust Gas Temperature Distribution in an Aircraft Piston Engine with and without a Turbocharger, Adv. Sci. Technol. Res. J., 2021, 15(3), 155–166, doi: 10.12913/22998624/139688.
12. Rajashekara K. Current and future trends in electrification of road and air transportation, iEnergy, 2023, 2(3), 159–160, doi: 10.23919/IEN.2023.0027
13. Delogu G, Porru M, Serpi A. A Brief Overview on Commercial Aircraft Electrification: Limits and Future Trends, in 2021 IEEE Vehicle Power and Propulsion Conference (VPPC), 2021; 1–5. doi: 10.1109/VPPC53923.2021.9699191.
14. Galiński C. Wybrane Zagadnienia Projektowania Samolotów, Wydawnictwa Naukowe Instytutu Lotnictwa, Warszawa 2016; 31–32, http://ilot.edu.pl/sklep/
15. Kozuba J, Wojnar T, Mrozik M, Stołtny B. Use of electric motors in the context. The classification of the electric propulsion' s elements in the motor gliders, 2021; 51(2), 103–116, doi: 10.2478/jok-2021-0025.
16. Jakliński P, Czarnigowski J, Ścisłowski K. Analysis of the operating conditions of the ASz-62IR engine during flight, Adv. Sci. Technol. Res. J., 2024; 18(8), 56–72, doi: 10.12913/22998624/192699.
17. Geiß I, Sizing of the energy storage system of hybrid-electric aircraft in general aviation, CEAS Aeronaut. J., 2017; 8(1), 53–65, doi: 10.1007/s13272-016-0220-5.
18. Friedrich C, Robertson P, Design of Hybrid-Electric Propulsion Systems for Light Aircraft, AIAA Aviation 2014 -14th AIAA Aviation Technology, Integration, and Operations Conference. doi: 10.2514/6.2014-3008.
19. Bravo GM, Praliyev N, Veress A, Performance Analysis of Hybrid Electric and Distributed Propulsion System Applied on a Light Aircraft Performance analysis of hybrid electric and distributed propulsion system applied on a light aircraft, Energy, 2020; 214, October, 118823, doi: 10.1016/j.energy.2020.118823.
20. Pawlak M, Kuźniar M. Performance and emission

of the aircraft with hybrid propulsion during take-off operation cycle, Adv. Sci. Technol. Res. J. 2024; 18(1), 155–166.

21. Kuźniar M, Pawlak M, Orkisz M, Comparison of Pollutants Emission for Hybrid Aircraft with Traditional and Multi-Propeller Distributed Propulsion, Sustainability, 2022; 14(22). doi: 10.3390/su142215076.
22. Kalwara M, Kuźniar M, Orkisz M, A rotating piston engine with electric generator in serial hybrid propulsion system for use in light aircraft, Combust. Engines, 2021; 187(4), 42–45. doi: 10.19206/CE-141353.
23. Nguyen DD, Kale U, Rohács D. Developing Models and Methods for Autonomous Drones in Urban Air Transport BT - Solutions for Maintenance Repair and Overhaul, T. H. Karakoc, J. Rohács, D. Rohács, S. Ekici, A. Dalkiran, and U. Kale, Eds., Cham: Springer International Publishing, 2024; 433–445.
24. Buican GR, Zaharia SM, Pascariu IS, Chicos LA, Lancea C, Pop MA, Stamate VM. Development And Implementation Of An Automated Pilot System For A Fixed-Wing Twin-Engine Airplane Uav. In Scientific Research and Education in the Air Force – AFASES Conference, 2022, Henri Coanda Air Force Academy, doi:10.19062/2247-3173.2022.23.23.
25. Pecho P, Velky P, Kapustik S, Novak A, Use of Computer Simulation to Optimize UAV Swarm Flying, in 2022 New Trends in Aviation Development (NTAD), 2022; 168–172. doi: 10.1109/NTAD57912.2022.10013577.
26. Czarnigowski J, Trendak M. Aircraft piston engine load distribution in steady state operating conditions, Combust. Engines, 2023; 193(2), 29–35, doi: 10.19206/CE-160505.